Comparing food web structures and dynamics across a suite of global marine ecosystem models

S.F. Sailley [a,*], M. Vogt [b], S.C. Doney [a], M.N. Aita [c], L. Bopp [d], E.T. Buitenhuis [e], T. Hashioka [c,e,f], I. Lima [a], C. Le Quéré [e], Y. Yamanaka [c]

[a] Department of Marine Chemistry and Geochemistry, Woods Hole Oceanographic Institution, Woods Hole, MA 02543, USA
[b] Institute for Biogeochemistry and Pollutant Dynamics, CHN 23.2, Universitatsstrasse 16, Ch-8092 Zürich, Switzerland
[c] Japan Agency for Marine-Earth Science and Technology, Yokohama, Japan
[d] Laboratoire du Climat et de l'Environnement (LSCE), L'Orme des Merisiers Bt. 712, 91191 Gif sur Yvette, France
[e] Tyndall Centre for Climate Change Research, School of Environmental Sciences, University of East Anglia, Norwich, UK
[f] Graduate School of Environmental Earth Science, Hokkaido University, Sapporo, Japan

ARTICLE INFO

ABSTRACT

Dynamic Green Ocean Models (DGOMs) include different sets of Plankton Functional Types (PFTs) and equations, thus different interactions and food webs. Using four DGOMs (CCSM-BEC, PISCES, NEMURO and PlankTOM5) we explore how predator–prey interactions influence food web dynamics. Using each model's equations and biomass output, interaction strengths (direct and specific) were calculated and the role of zooplankton in modeled food webs examined. In CCSM-BEC the single size-class adaptive zooplankton preys on different phytoplankton groups according to prey availability and food preferences, resulting in a strong top-down control. In PISCES the micro- and meso-zooplankton groups compete for food resources, grazing phytoplankton depending on their availability in a mixture of bottom-up and top-down control. In NEMURO macrozooplankton controls the biomass of other zooplankton PFTs and defines the structure of the food web with a strong top-down control within the zooplankton. In PlankTOM5, competition and predation between micro- and meso-zooplankton along with strong preferences for nanophytoplankton and diatoms, respectively, leads to their mutual exclusion with a mixture of bottom-up and top-down control of the plankton community composition. In each model, the grazing pressure of the zooplankton PFTs and the way it is exerted on their preys may result in the food web dynamics and structure of the model to diverge from the one that was intended when designing the model. Our approach shows that the food web dynamics, in particular the strength of the predator–prey interactions, are driven by the choice of parameters and more specifically the food preferences. Consequently, our findings stress the importance of equation and parameter choice as they define interactions between PFTs and overall food web dynamics (competition, bottom-up or top-down effects). Also, the differences in the simulated food-webs between different models highlight the gap of knowledge for zooplankton rates and predator–prey interactions. In particular, concerted effort is needed to identify the key growth and loss parameters and interactions and quantify them with targeted laboratory experiments in order to bring our understanding of zooplankton at a similar level to phytoplankton.

© 2013 The Authors. Published by Elsevier B.V.

1. Introduction

Changes in marine ecosystem structure and functioning, due to anthropogenic greenhouse gas emissions and climate change, have created a need for more detailed marine ecosystem models in order to forecast potential climate and ocean acidification impacts (e.g., changes in biogeochemical cycles, carbon dioxide sinks and sources, biological community composition, Doney et al., 2009a, 2012). Dynamic Green Ocean Models (DGOMs) were developed from the need to understand how changing conditions affect lower trophic marine food-webs (i.e., plankton), and the biogeochemical cycles organisms are linked to. The inclusion of biological complexity and functional diversity has been achieved through the use of Plankton Functional Types (PFTs) for both phytoplankton (pPFT) and zooplankton (zPFT) (Falkowski et al., 2000; Moore et al., 2004; Le Quéré et al., 2005). A PFT can be defined by the role it

* Corresponding author at: Woods Hole Oceanographic Institution, 266 Woods Hole Road, Woods Hole, MA 02543, USA. Tel.: +1 508 289 3486.
E-mail addresses: ssailley@yahoo.fr, ssailley@whoi.edu (S.F. Sailley).

plays in the biogeochemical cycle of specific elements (e.g., diatoms and the silica cycle), and in processes such as remineralization (e.g., bacteria), grazing and export mediated through size class (e.g. microzooplankton versus mesozooplankton PFTs, (Le Quéré et al., 2005)).

Model output (e.g. PFT biomass, distribution, export) is often sensitive to small changes in model parameters (Woods and Thomas, 1999; Fussmann and Balsius, 2005) and the modeled functional forms (Anderson, 2005). In comparison to phytoplankton–zooplankton–nutrient models (NPZD; Fasham et al., 1993), DGOMs present an increase in complexity through a larger number of compartments as well as explicit biogeochemical cycles (e.g. C, N, P, Si). Consequently, there are a greater number of equations and parameters that have to be chosen carefully so as to describe best the group of organisms they represent. Formulations for zooplankton are particularly important in this regard due to their effect on several processes: phytoplankton mortality due to zooplankton grazing, export of carbon through feces production, food sources for higher trophic levels (e.g., larger zooplankton, fish, marine mammals, birds).

However, PFTs and size class are loose guidelines and deciding on the optimal structure of the food web and the functional responses is left to the modeler judgement; this lead to a variety of DGOMs. To understand and map the variety of the existing DGOMs, the MARine Ecosystem Intercomparison Project (MAREMIP, http://maremip.uea.ac.uk) aims at comparing food web functioning in different DGOMs. The DGOMs available in the first stage of the project are CCSM-BEC (Moore et al., 2004; Doney et al., 2009b), PISCES (Aumont and Bopp, 2006), NEMURO (Kishi et al., 2007) and PlankTOM5 (Buitenhuis et al., 2010). The four DGOMs describe marine ecosystems using different PFTs, equations and parameters, which, as stated earlier, significantly impact model outputs (e.g. PFT biomass, export, respiration). As such we have four different ecosystem structure and different ocean physics. We are comparing different integrated systems.

Even when concentrating on the biological part, the definition of PFTs within a model creates flexibility in how they are defined. This is especially true for zooplankton, where generic size class regroup a variety of organisms and behavior. Consequently comparison of zooplankton between models is made difficult by the lack of common metrics. The smallest common denominator for zooplankton is the functional response (grazing equation and parameter value), which impact the model dynamics. However, this was never explored in details as long as the modeled primary production and export are comparable to observations. Thus, comparing both the equations and the outputs of DGOMs is bound to improve our understanding of zooplankton parameterization and its influence on model results beyond agreement with observations.

The goal of this paper is to compare zooplankton and their trophic interactions as well as how they shape the model food web using three model aspects: (i) model parameterization (formulation, maximal rates and food preferences); (ii) the relationship of simulated predator and prey biomasses; and (iii) the interaction strength between PFTs with a focus on predator–prey interactions. The intent is not to establish a ranking of the available models, but look at them with a new set of tool.

2. Methods

2.1. Data

We use PFT biomasses from the available DGOMs (CCSM-BEC, Moore et al., 2004; Doney et al., 2009a,b; PISCES, Aumont and Bopp, 2006; PlankTOM5, Buitenhuis et al., 2010; and NEMURO, Aita et al., 2007). Data are regridded onto a 360×180 pixels grid and binned into 5×5 degree bins. Annual means of surface data are used to compare PFT biomass. We also use observations of biomass for microzooplankton and mesozooplankton from Buitenhuis et al. (2006, 2010). Detrital particulate organic carbon (POC) is also a food source for zooplankton, but this compartment is neglected, since food preferences for POC are lower than those for pPFT or other zPFT in all models.

2.2. Holling type and Ivlev grazing functional forms

The DGOMs use different grazing functional forms. CCSM-BEC uses a Holling type III (sigmoidal equation; Eq. (1)), PISCES and PlankTOM5 use a Holling type II (Monod equation; Eq. (2)) and NEMURO an Ivlev equation (Eq. (3)):

$$G_{H_3} = g \times T_f \times \frac{F^2}{k^2 + F^2} \tag{1}$$

$$G_{H_2} = g \times T_f \times \frac{F}{k + F} \tag{2}$$

$$G_{Ivlev} = g \times T_f \times (1 - e^{(-F/k)}) \tag{3}$$

G is the specific grazing rate (d^{-1}), g is the maximal grazing rate (d^{-1}) at a reference temperature, T_f is a temperature function, k is the half saturation concentration ($mmol\,C\,m^{-3}$) and F the prey concentration ($mmol\,C\,m^{-3}$). For each of these equations grazing starts to saturate at a prey concentration of about $2k$. The Holling type III equation creates what is called a refuge from grazing at low prey concentration that is absent in the Holling type II equation. The equations used are shown in their basic forms, and additional parameters can be used to include prey preference, grazing threshold or toxicity of the prey (Gentleman et al., 2003).

2.3. DGOMs: equation and parameters

Each of the DGOMs analyzed here includes at least 2 phytoplankton PFTs (Table 1): nanophytoplankton (S, all DGOMs) and diatoms (D, all DGOMs); additional pPFTS are diazotrophs (N, CCSM-BEC) and coccolithophores (C, PlankTOM5). CCSM-BEC only has a single generic zooplankton (Z_G), while PISCES ad PlankTOM5 have two zooplankton PFTs: microzooplankton (Z) and mesozooplankton (M); NEMURO has a third zooplankton PFT: predatory zooplankton or macrozooplankton (P). An analysis of the phytoplankton distribution, dominance patterns and ecological niches is presented in Vogt et al. (in preparation) and an analysis of spring bloom dynamics in Hashioka et al. (under review). Note that the food web structure of each DGOM can be seen in Fig. 12a.

2.3.1. CCSM-BEC

In CCSM-BEC the specific grazing rate equation for Z_G on all three pPFTs (F) uses a Holling type III function (Table 2). CCSM-BEC's zooplankton is generic and food preferences are expressed in the different g^F values depending on pPFT. The scaling factor (f^F) for grazing on diatoms lowers the concentration at which grazing on diatoms reaches its maximum. According to g^F and f^F, zooplankton food preference decreases from nanoflagellates, to diatoms and then diazotrophs.

2.3.2. PISCES

The grazing equation for specific grazing rate (d^{-1}) in PISCES is a Holling type II with prey preferences; the formulation is independent of the prey (F, Table 2). Microzooplankton has a higher maximal grazing rate than mesozooplankton, so at equal biomass the grazing impact of microzooplankton on phytoplankton is higher than that of mesozooplankton. Also, microzooplankton

Table 1
PFT for each DGOMs. With S: nanophytoplankton, D: diatoms, N: diazotrophs, C: coccolithophores, Z_G: generic zooplankton, Z: microzooplankton, M: mesozooplankton, P: macrozooplankton.

		CCSM-BEC	PISCES	NEMURO	PlankTOM5
Phytoplankton	S	X	X	X	X
	D	X	X	X	X
	N	X			
	C				X
Zooplankton	Z_G	X			
	Z		X	X	X
	M		X	X	X
	P			X	

has equal prey preferences for nanophytoplankton and diatoms while mesozooplankton has a marked preference for diatoms and microzooplankton over nanophytoplankton.

2.3.3. NEMURO

NEMURO's grazing formulation uses an Ivlev equation that depends on the prey-predator pair (Table 2). Microzooplankton and mesozooplankton have no prey preferences *per se*, just different maximal grazing rates. The macrozooplankton grazing equation includes an additional prey preference or, as qualified by Kishi et al. (2007) a "gourmet function" ($e^{(f^P_{prey})}$, Table 2). The gourmet function inhibits grazing on a prey if the preferred preys are available. As a result, the gourmet function gives macrozooplankton a preference for zooplankton over diatoms, and for mesozooplankton over microzooplankton. Note that the gourmet function is equal to one (f^P_{prey}=0) for grazing of macrozooplankton on mesozooplankton, and for grazing by mesozooplankton and microzooplankton on any prey.

2.3.4. PlankTOM5

The grazing equation in PlankTOM5 is similar to the one in PISCES (Holling type II, Table 2). Microzooplankton has a preference for nanophytoplankton over coccolithophores over diatoms.

Mesozooplankton has an equal and marked preference for diatoms and microzooplankton as primary food sources. Microzooplankton maximal grazing rate is greater than mesozooplankton maximal grazing rate, and grazing saturation occurs at higher prey biomass for microzooplankton than for mesozooplankton ($k^Z \gg k^M$) making microzooplankton a more efficient grazer at high prey biomass.

2.4. Interaction strength (IS)

The Jacobian matrix (J), or community matrix (May, 1974), is composed of the partial derivatives of the growth equation of one organism as a function of a change in the biomass of another organism. The individual terms in the Jacobian define the direct interaction strength (dIS) between a pair of organisms Y and X (dIS$_{Y-X}$, Eq. (4)).

$$\text{dIS}_{Y-X} = \frac{\partial}{\partial Y}\frac{\partial X}{\partial t} \tag{4}$$

dIS$_{Y-X}$ has units of (Xbiomass)(Ybiomass)$^{-1}$(time)$^{-1}$ and expresses the impact a change in biomass of a group of organisms (Y) has on the time rate of change of another group of organisms (X) through direct (e.g., grazing) interaction. In the case of a PZ_1Z_2

Table 2
Formulation of grazing functional response and parameter value for each model. With S: nanophytoplankton, D: diatoms, N: diazotrophs, C: coccolithophores, Z_G: generic zooplankton, Z: microzooplankton, M: mesozooplankton, P: macrozooplankton.

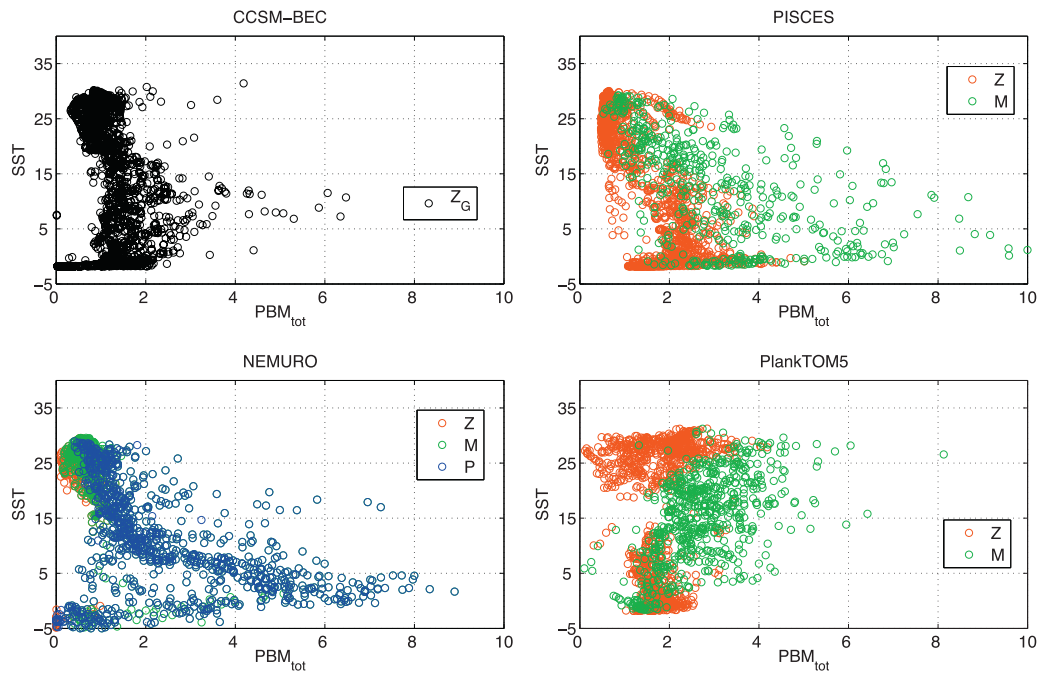| Model	zPFT	pPFT	Grazing equation	g (d^{-1}, at 0 °C)	K or λ (mmol C m^{-3})	Other	Q_{10}
CCSM-BEC	Z_G	S		0.34	1.05	$f^F = 1$	
		D	$G(F) = g^F T_f \left(\frac{F^2}{F^2 + k^2 f^F}\right)$	0.26	1.05	$f^F = 0.81$	2
		N		0.15	1.05	$f^F = 1$	
PISCES	Z	S		4	20	$p^Z_S = 0.5$	
	Z	D		4	20	$p^Z_D = 0.5$	
	M	S	$G^{zPFT}(F) = g^{zPFT} T_f \frac{p^{zPFT}_F F}{k^{zPFT} + \sum_F (p^{zPFT}_F F)}$	0.7	20	$p^M_S = 0.2$	1.9
	M	D		0.7	20	$p^M_D = 1$	
	M	Z		0.7	20	$p^M_Z = 1$	
NEMURO	Z	S		0.4	1.4	$f^P_{prey} = 0$	
	M	S		0.1	1.4	$f^P_{prey} = 0$	
	M	D		0.4	1.4	$f^P_{prey} = 0$	
	M	Z	$G^{zPFT}(F) = g^{zPFT}_F \times T_f \times \{1 - e^{(-(F - p2z^*)\lambda)}\} \times e^{(f^P_{prey})}$	0.4	1.4	$f^P_{prey} = 0$	2
	P	D		0.2	1.4	$f^P_{prey} = -\psi_D(M + Z)$	
	P	Z		0.2	1.4	$f^P_{prey} = -\psi_Z \times M$	
	P	M		0.2	1.4	$f^P_{prey} = 0$	
					Value in μmol N l^{-1}	C:N ratio of 133:17	$\psi_D = 4.605$
							$\psi_Z = 3.01$
PlankTOM5	Z	S		0.92	6.4	$p^Z_S = 1.29$	1.71
	Z	D		0.92	6.4	$p^Z_D = 0.26$	1.71
	Z	C		0.92	6.4	$p^Z_C = 1.03$	1.71
	M	S	$G^{zPFT}(F) = g^{zPFT} T_f \frac{p^{zPFT}_F F}{k^{zPFT} + \sum_F p^{zPFT}_F F}$	0.3	0.26	$p^M_S = 0.51$	1.77
	M	D		0.3	0.26	$p^M_D = 2.54$	1.77
	M	C		0.3	0.26	$p^M_C = 0.63$	1.77
	M	Z		0.3	0.26	$p^M_Z = 2.54$	1.77

Fig. 1. Ecological niches for zooplankton functional types (zPFTs) depending on total phytoplankton biomass (PBM$_{tot}$, in mmol C m^{-3}) and sea surface temperature (SST). The plot presents the dominant zPFT (biomass $\geq$50% of total zooplankton biomass) for the annual mean in 5 × 5 bin. Z_G: generic zooplankton in CCSM-BEC (black), Z: microzooplankton (red), M: mesozooplankton (green), and P: macrozooplankton (blue).

food web, with P the prey for Z_1 and Z_2, and Z_2 grazing on Z_1 as well, we have a 3 × 3 Jacobian (J):

$$J = \begin{bmatrix} \text{dIS}_{P-P} & \text{dIS}_{Z_1-P} & \text{dIS}_{Z_2-P} \\ \text{dIS}_{P-Z_1} & \text{dIS}_{Z_1-Z_1} & \text{dIS}_{Z_2-Z_1} \\ \text{dIS}_{P-Z_2} & \text{dIS}_{Z_1-Z_2} & \text{dIS}_{Z_2-Z_2} \end{bmatrix}$$

The terms dIS$_{Z_1-P}$, dIS$_{Z_2-P}$ and dIS$_{Z_2-Z_1}$ above and to the right of the diagonal are the impact of changes in predator biomass on the time rate of change of the prey and are expected to be negative; while the impact of prey on predator (dIS$_{P-Z_1}$, dIS$_{P-Z_2}$ and dIS$_{Z_1-Z_2}$, below and to the left of the diagonal) are expected to be positive. In addition to the interaction sign, numerical solutions of the derivatives give the interaction strengths between organism pairs and determine the strongest interactions within the food web.

For each DGOM, the analytical solutions for each term in the Jacobian matrix (J) are constructed based on the growth equations for the PFTs (Laska and Wootton, 1998); then biomass and parameter values are substituted into the analytical solutions to give numerical estimates for the dIS (e.g., grazing interaction) between PFTs. DGOMs are dynamic systems, and as a consequence, PFT biomass varies in time and space and dIS will also vary with biomass, temperature, etc. We focus on dIS$_{predator-prey}$ as a function of biomass. The biomass of the prey and predator PFTs are considered through their modeled biomass range, while biomass of other PFTs (if affecting dIS) are considered as fixed at their median value. Therefore dIS values are illustrative of the predator–prey interaction; if another PFT biomass has a significant impact on the dIS value it is not directly visible.

It is noteworthy that while the interaction strength concept is widely used and known in theoretical ecology and applied to real community, with varied level of consensus (Berlow et al., 2004; Wootton and Emmerson, 2005), to the knowledge of the authors it has not been applied to DGOMs.

3. Results

3.1. Ecological niches

The dominant zPFTs (accounting for more than 50% of the total zooplankton biomass) for each model grid cell are plotted as a function of annual average sea surface temperature (SST) and total phytoplankton biomass (PBM$_{tot}$, Fig. 1) to visualize the ecological niche of each zPFTs. We plot the dominant zPFT and not their presence because PFT extinction is prevented, and are thus present everywhere even if at low concentration. In addition, visualizing the dominant zPFT shows possible specialization of one zPFT. Note that CCSM-BEC only possesses a generic zooplankton and its niche is equivalent to a map of the total pPFT biomass plotted against SST.

In CCSM-BEC, the generic zooplankton group is present in the full SST range from −2 to 30 °C, for total phytoplankton concentrations below 2 mmol C m^{-3}; they are also present for higher phytoplankton biomass levels between 5 and 15 °C and above 25 °C. In PISCES, microzooplankton is dominant where phytoplankton total biomass is around 1 mmol C m^{-3} and SST above 15 °C, or for a phytoplankton biomass of about 2.5 mmol C m^{-3} for SSTs below 15 °C. For most SSTs, mesozooplankton is dominant at higher total phytoplankton biomass, but the niches of both zPFTs overlap. In NEMURO, the area of dominance of the zPFTs overlap with three main niches: for a temperature around 25 °C at phytoplankton total biomass below 1 mmol C m^{-3}, around 3–5 °C and phytoplankton biomass ranging from 3 to 8 mmol C m^{-3}, and for low temperature (0 to −5 °C) with phytoplankton biomass below 4 mmol C m^{-3}; there is also a band from 7 to 25 °C for phytoplankton biomass below 2 mmol C m^{-3}. The overlap between the ecological niches of the three zPFTs indicates that all zPFTs are tightly bound to each other (strong interaction) and to the pPFTs as well. In PlankTOM5, microzooplankton dominates for temperatures above 20 and below 14 °C and for a total phytoplankton biomass around and below 2 mmol C m^{-3}. Mesozooplankton is dominant for temperatures between 5 and 25 °C and phytoplankton total
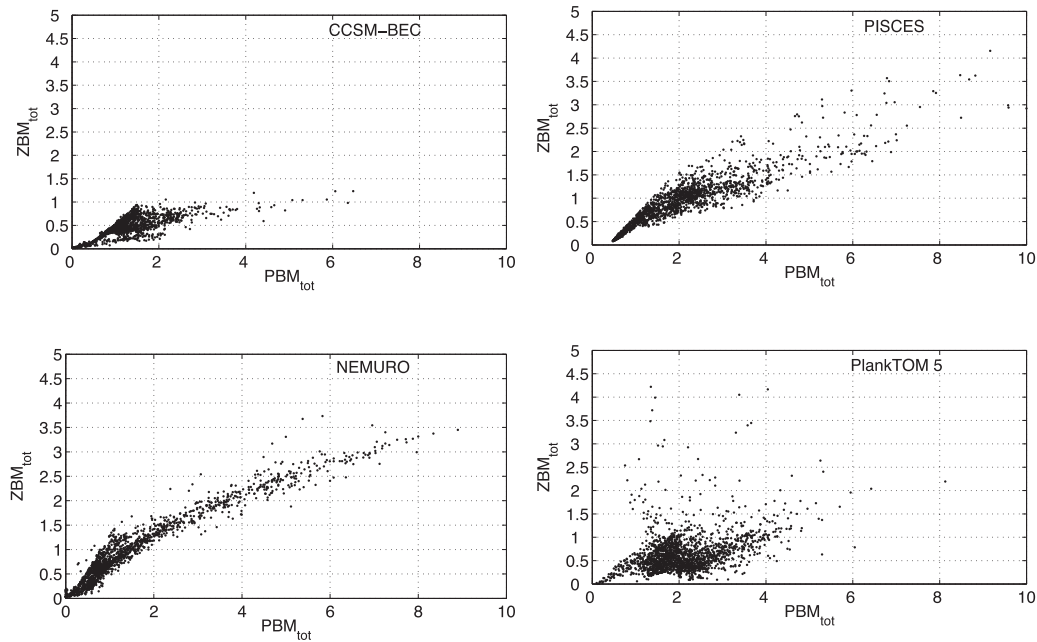
Fig. 2. Variation of total zooplankton biomass (ZBM$_{tot}$) with total phytoplankton biomass (PBM$_{tot}$). Biomass represents abundance in mmol C m^{-3}.

biomass above 2 mmol C m^{-3}; there is little to no overlap between the niches of the two zPFTs.

3.2. Trophic levels

Using annual surface average biomass, the relationship between predator and prey biomass for the four DGOMs are shown in Fig. 2. In PISCES and NEMURO the shape of the grazing equation (Monod equation and Ivlev, respectively) is more evident at low prey concentration than in CCSM-BEC and PlankTOM5. In CCSM-BEC and PlankTOM5, at high phytoplankton biomass ($\geq$1 mmol C m^{-3}) the total zooplankton biomass is mostly independent of the total phytoplankton biomass, and in CCSM-BEC it does not increase past a maximal value in an apparent saturation of the grazing. Total zooplankton biomass in PISCES and NEMURO present a continuous increase of zooplankton biomass with increasing phytoplankton biomass, indicating a different balance between grazing and loss processes for the models, compared to CCSM-BEC and PlankTOM5.

In addition, the maximal zooplankton biomass reached differs between all four models, in increasing order of maximal value: about 1 mmol C m^{-3} in CCSM-BEC; 3.5 mmol C m^{-3} in NEMURO; and approximately 4 mmol C m^{-3} in PISCES and PlankTOM5 (Fig. 3).

The variation of the simulated biomass of the largest zooplankton class (mesozooplankton in PlankTOM5 and PISCES, macrozooplankton in NEMURO) compared to that of microzooplankton is a clue to the dynamics among zPFTs (Fig. 4). While there are not enough observations (Buitenhuis et al., 2006, 2010) to determine whether there is a natural relationship between microzooplankton and larger zooplankton biomass, different relationships are visible for DGOMs that include more than one zPFT. In PISCES, mesozooplankton biomass increases non-linearly with increasing microzooplankton biomass, and a larger maximal biomass is reached for mesozooplankton than for microzooplankton (2.5 and 1.3 mmol C m^{-3}, respectively). In NEMURO, microzooplankton biomass does not increase past 0.5 mmol C m^{-3} (but for a few outliers at 0.7 mmol C m^{-3}), and macrozooplankton
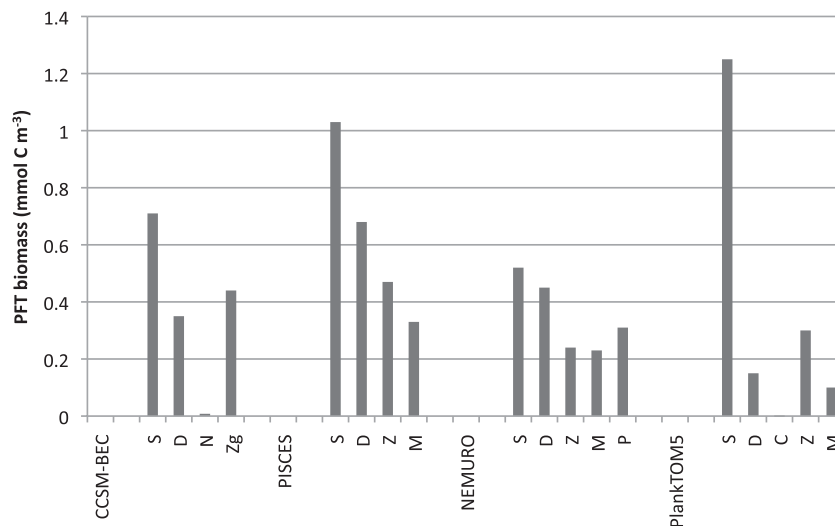

Fig. 3. Median biomass (mmol C m^{-3}) for the various plankton functional types (PFTs) of each model. *S*: nanophytoplankton, *D*: diatoms, *N*: diazotrophs, *C*: coccolithophores, *Z$_G$*: generic zooplankton, *Z*: microzooplankton, *M*: mesozooplankton, *P*: macrozooplankton.
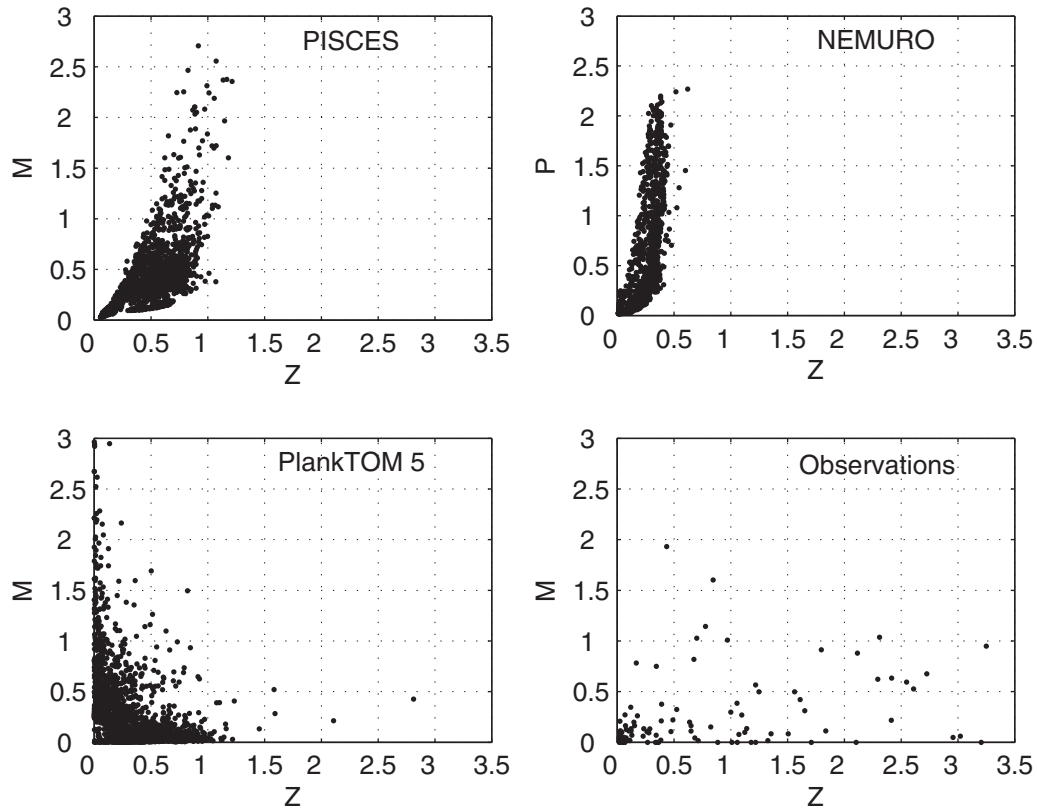
Fig. 4. Variation of top predator biomass (mesozooplankton 'M' or macrozooplankton 'P') with microzooplankton (Z) biomass. Biomass represents abundance in mmol C m^{-3} (Buitenhuis et al., 2006, 2010).

biomass levels reach above 2 mmol C m^{-3}. In PlankTOM5, mesozooplankton and microzooplankton coexist only in conditions with low biomass for each zPFT; higher values of one zPFT appear to occur only where the other zPFT is excluded.

3.3. PFTs biomass and direct interaction strength, dIS$_{predator–prey}$

The distribution and biomass of a zPFT are governed in part by its grazing formulation, food preferences and prey abundances: pPFTs and smaller zPFTs. This is illustrated by the dIS dependence on biomass. dIS$_{predator–prey}$ can depend on the prey biomass only, on the prey and predator biomass or on the biomass of another PFT which is not part of the predator–prey pair. Fig. 4 illustrates the different median PFT biomass values within and between models (values used in obtaining numeric values for dIS$_{predator–prey}$). Fig. 5a illustrates dIS$_{predator–prey}$ at climatological annual surface median biomass (biomass effect on dIS not visible) and highlights the strongest interaction within the models (highest absolute dIS$_{predator–prey}$). In some models (especially CCSM-BEC and PISCES) the predator biomass increase almost linearly with the prey biomass, and the dIS$_{predator–prey}$ variation in these models depends on the prey biomass only (i.e. the biomass of other PFTs are not part of the equation), or variations in dIS$_{predator–prey}$ due to variations in the biomass of other PFTs are negligible. The resulting effects of biomass variation on each dIS$_{predator–prey}$ are explored in more detail in Figs. 6–11 and Eqs. (5)–(17) that are a result from the Jacobian analytical solution. These figures display the variation of predator–prey annual mean surface biomass from model output, and dIS curves are overlain to show how biomass influences predator–prey interactions. The temperature effect on rates is ignored by using the model reference temperature (0 °C) for grazing and growth rates, especially considering that temperature

dependence of grazing rates is the same between zPFTs within each models (except for PlankTOM5, where the difference is small enough that it could be ignored). Table 3 includes minimal, maximal and median value for the dIS$_{predator–prey}$.

3.3.1. CCSM-BEC

In CCSM-BEC, dIS$_{Z_G-F}$ is dependent on the prey biomass (F) only (Fig. 6, Eq. (5)) and the absolute value of dIS$_{Z_G-pPFT}$ increases monotonically with prey biomass.

$$\text{dIS}_{Z_G-F} = -F^2 \times \frac{g^F}{F^2 + f^F k^2} \tag{5}$$

The biomass of the generic zooplankton increases with nanophytoplankton and diatom biomass (Fig. 6a and b); there is no evident variation of the generic zooplankton biomass with that of the diazotrophs (Fig. 6c). For both dIS$_{Z_G-D}$ and dIS$_{Z_G-S}$, the dIS$_{Z_G-prey}$ values are between 0 and −0.3, becoming larger in an absolute sense with increasing phytoplankton biomass. $Z_G - D$ biomass pairs are mostly in a range where dIS$_{Z_G-D}$ will be between 0 and −0.2 (Fig. 6b). For the $Z_G - S$ biomass pairs, dIS$_{Z_G-S}$ values typically range between −0.1 and −0.3 (Fig. 6a). The larger absolute values mean that dIS$_{Z_G-S}$ is generally stronger than dIS$_{Z_G-D}$. dIS$_{Z_G-N}$ is between 0 and −0.02 (Fig. 6c), making it the weakest interaction in CCSM-BEC (this is partly due to the low biomass of nitrogen fixers). The emerging pattern, as expected from the grazing formulation, is one where the generic zooplankton indiscriminately graze on all three pPFTS, where the grazing pressure and dIS$_{predator–prey}$ depends on the prey biomass only.

3.3.2. PISCES

In PISCES, the dIS values are dependent on prey biomass (F) and, due to the food preference formulation, other prey can have
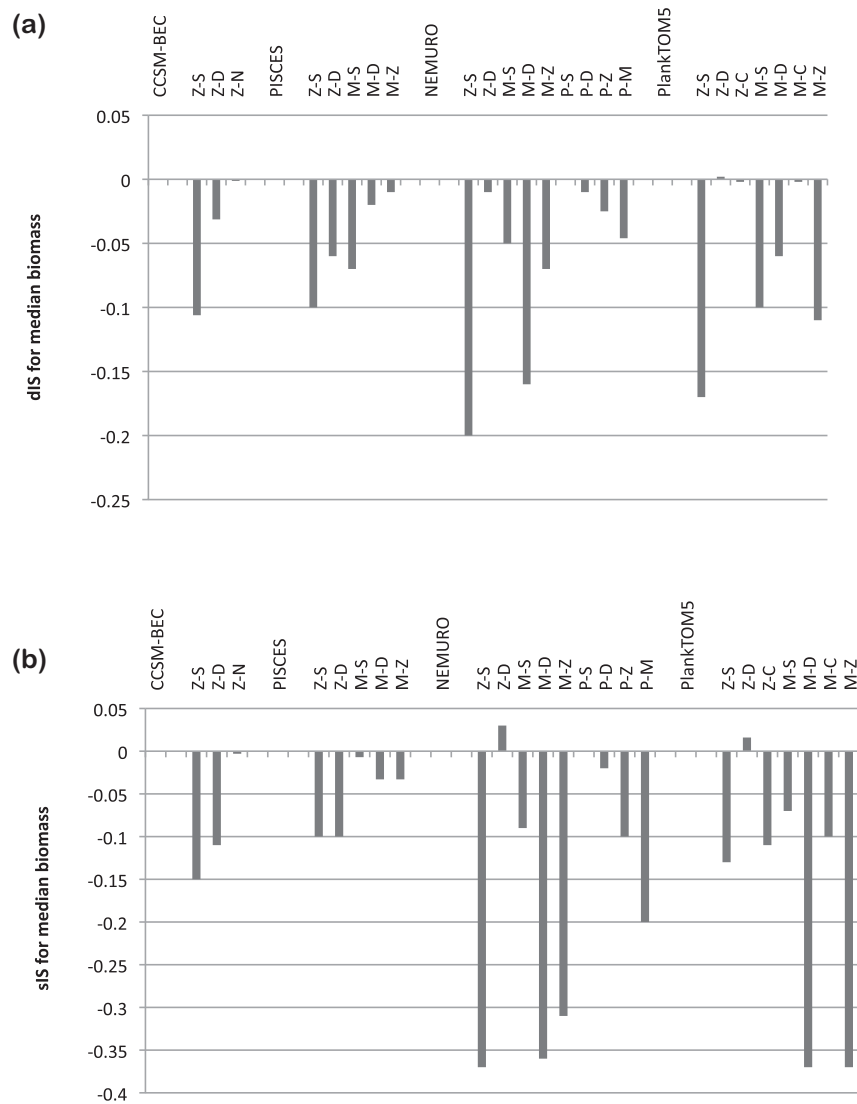
Fig. 5. (a) Direct interaction strength ($dIS_{predator–prey}$) at median plankton functional type (PFT) biomass for each model. The $dIS_{predator–prey}$ have a unit of (prey biomass)(predator biomass)$^{-1}$ time^{-1}. (b) Specific interaction strength ($sIS_{predator–prey}$) at median PFT biomass for each model. Unit of predator biomass^{-1} time^{-1}.

an impact on the $dIS_{predator–prey}$ values. For microzooplankton, the equation describing $dIS_{Z–F}$ is composed of two terms (Eq. (6)):

$$dIS_{Z-F} = -F \frac{g^Z p_F^Z}{k^Z + \sum F p_F^Z} + MF \frac{g^M p_F^M p_Z^M}{(k^M + \sum F p_F^M)^2} \quad (6)$$

The first, negative, term in the equations is the direct impact of microzooplankton grazing on its prey. The second term is the impact of microzooplankton abundance through mesozooplankton grazing due to the food preference formulation (i.e., a change in microzooplankton biomass will change the grazing pressure of mesozooplankton on pPFTs). The first part of the equations depends mostly on prey biomass, and the second term on both prey and mesozooplankton biomass. The first term of the equation is however dominant, and even if the equations permit high mesozooplankton biomass to weaken $dIS_{Z–F}$ this is not realized in the range of biomasses simulated by the model.

For mesozooplankton there is only one term to the equations describing $dIS_{M–F}$ (Eq. (7)):

$$dIS_{M-F} = -F \frac{g^M p_F^M}{k^M + \sum F p_F^M} \quad (7)$$

$dIS_{M–F}$ depends on prey biomass, although the equation structure allows for microzooplankton biomass to influence $dIS_{M–D}$ and for diatom biomass to influence $dIS_{M–Z}$. This is due to p_F^M being equal for microzooplankton and diatoms. Since diatom biomass is higher than microzooplankton biomass, in the model, it will slightly weaken $dIS_{M–Z}$, but microzooplankton biomass will not significantly weaken $dIS_{M–D}$.

Variation of zPFT biomass, and of $dIS_{predator–prey}$, with pPFT biomass is almost linear (Fig. 7). $dIS_{zPFT–S}$ depends on nanophytoplankton biomass; increasing nanophytoplankton biomass means an increase in the absolute value of $dIS_{zPFT–S}$ (Fig. 7a and c). At any fixed nanophytoplankton biomass, $dIS_{Z–S}$ is stronger than $dIS_{M–S}$, with maximum "absolute" values of −0.25 and −0.15, respectively. As with nanophytoplankton, $dIS_{zPFT–D}$ absolute value depends on diatom biomass and will increase with increasing diatom biomass (Fig. 7b and d). Similarly to $dIS_{zPFT–S}$, at any fixed diatom biomass, $dIS_{Z–D}$ will be stronger than $dIS_{M–D}$ (maximum "absolute" dIS of −0.4 and −0.12, respectively). In addition, diatom biomass typically exceeds microzooplankton biomass, which are an equally preferred prey for mesozooplankton. As a result diatom biomass can weaken $dIS_{M–Z}$ (Fig. 7f for effect of diatom biomass on $dIS_{M–Z}$, and Fig 7e for $dIS_{M–Z}$ as function of microzooplankton
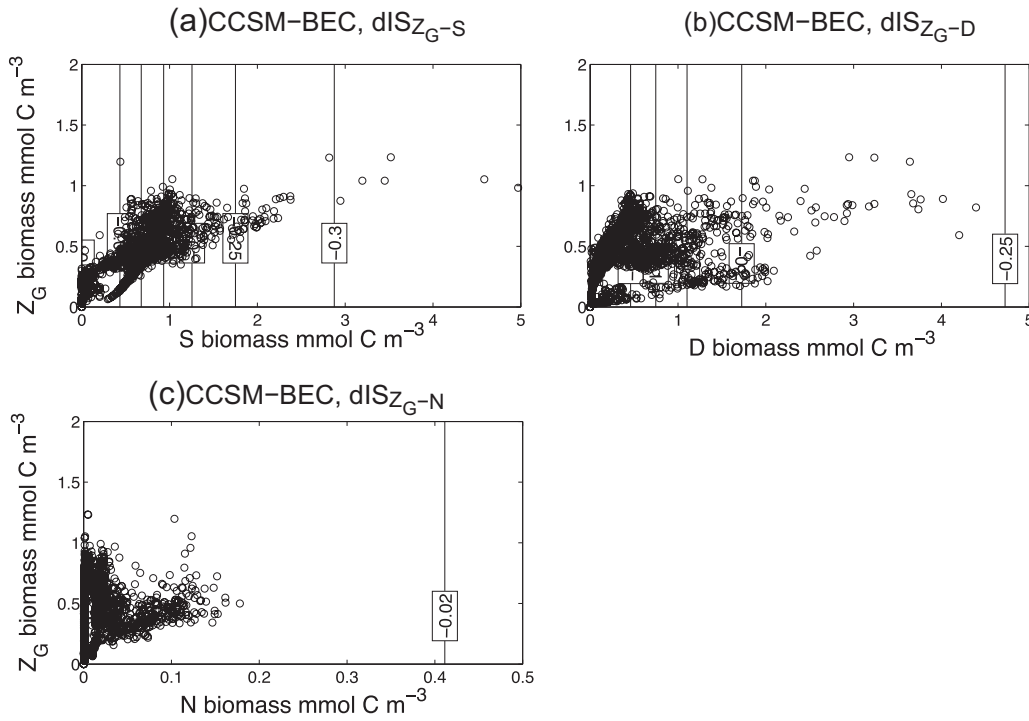
Fig. 6. CCSM-BEC: variation of generic zooplankton biomass (Z_G) with prey biomass: (a) nanophytoplankton (S), (b) diatom (D) and (c) diazotrophs (N) in mmol C m^{-3} (circle), and variation of dIS$_{Z_G-prey}$ as a function of the biomass (contour line, in (prey biomass)(predator biomass)$^{-1}$ time^{-1}).

and mesozooplankton), which is PISCES weakest dIS$_{predator-prey}$ (maximal "absolute" value reached of −0.04). This indicates that grazing pressure of both zPFTs is dependent foremost on the pPFT biomass, then on the food preferences. The emerging pattern is

that of co-existence and competition of both zPFTs: they prey on pPFTs according to their biomass, but the advantage of microzooplankton as a more efficient grazer is balanced by the grazing pressure exerted by mesozooplankton on microzooplankton.
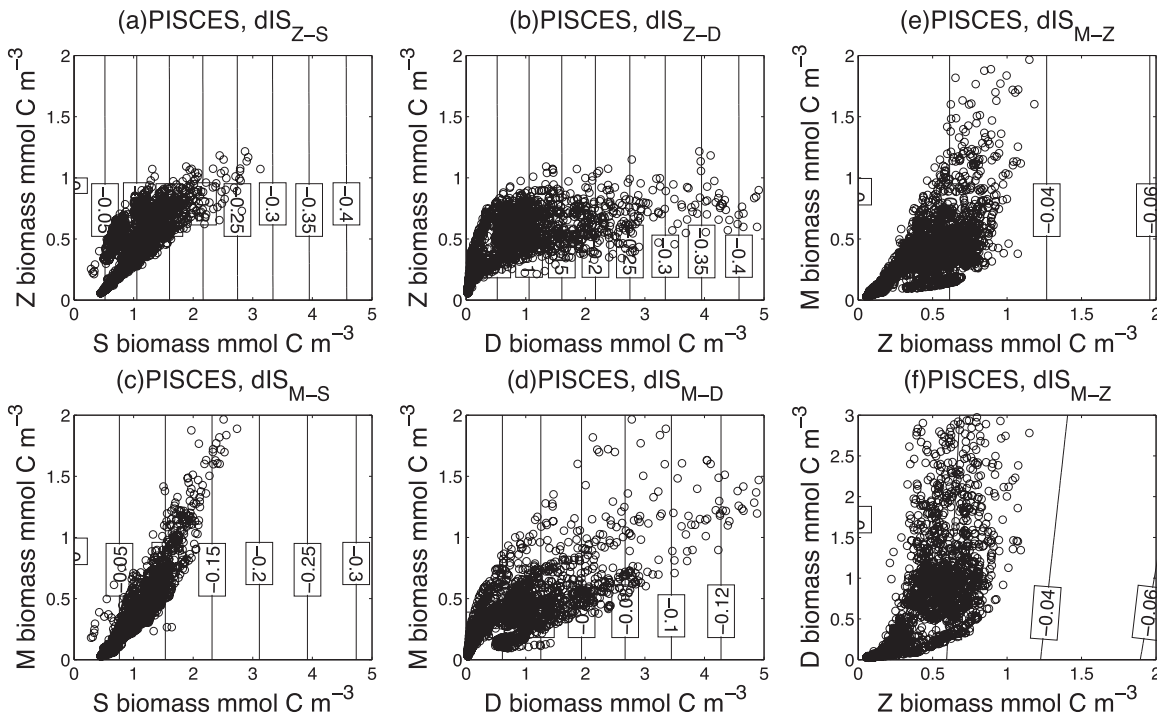

Fig. 7. PISCES: (a) and (b) variation of microzooplankton biomass (Z) with prey biomass (nanophytoplankton (S) and diatoms (D)) in mmol C m^{-3} (circle) and variation of dIS$_{Z-prey}$ as a function of the biomass (contour line, in (prey biomass)(predator biomass)$^{-1}$ time^{-1}). (c) to (e) variation of mesozooplankton biomass (M) with prey biomass (nanophytoplankton (S), diatom (D) and microzooplankton (Z)) in mmol C m^{-3} (circle) and variation of dIS$_{M-prey}$ as a function of the biomass (contour line, in (prey biomass)(predator biomass)$^{-1}$ time^{-1}). (f) Variation of dIS$_{M-Z}$ as a function of diatoms (D) and microzooplankton (Z) biomass showing how high diatom biomass will slightly weaken dIS$_{M-Z}$.
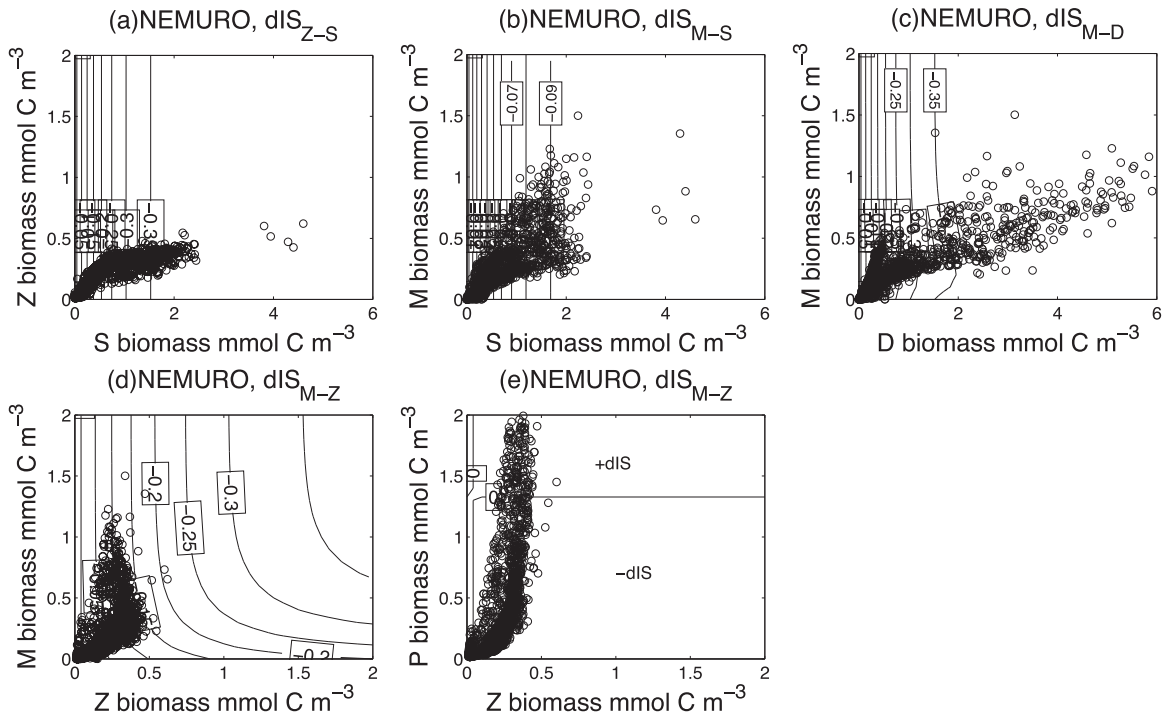
Fig. 8. NEMURO: (a) and (b) variation of zooplankton biomass (microzooplankton (Z) and mesozooplankton (M)) with nanophytoplankton biomass (S) in mmol C m^{-3} (circle) and variation of dIS$_{predator-S}$ as a function of the biomass (contour line, units given as (prey biomass) (predator biomass)$^{-1}$ time^{-1}). (c) Variation of dIS$_{M-D}$ (contour line, in (prey biomass) (predator biomass)$^{-1}$ time^{-1}) as a function of mesozooplanton (M) and diatoms (D) biomass (circle, in mmol C m^{-3}). (d) and (e) variation of dIS$_{M-Z}$ (contour line, in (prey biomass) (predator biomass)$^{-1}$ time^{-1}) as a function of (d) mesozooplankton (M) and microzooplankton (Z) biomass (circle, in mmol C m^{-3}) and (e) macrozooplankton (P) and microzooplankton (Z) biomass (circle, in mmol C m^{-3}); in (e) "+dIS" and "−dIS" give the sign of dIS for the area they are in, since the numerical value of dIS is negligible (1×10^{-4}).

3.3.3. NEMURO

In NEMURO, the dIS$_{predator-prey}$ terms are primarily dependent on prey biomass. For macrozooplankton, the additional "gourmet function" (Table 2) adds a dependence of dIS$_{P-prey}$ on the biomass of the other potential prey. This formulation also adds an extra term to dIS$_{M-D}$ and dIS$_{M-Z}$, as well as dIS$_{Z-D}$ (Eq. (8)) even though microzooplankton does not graze on diatoms:

$$\text{dIS}_{Z-D} = g_D^P \, P \, \psi_D \left[1 - \frac{1}{e^{(\lambda_P (D - p2z^*))}} \right] \times \frac{1}{e^{(\psi_D (M+Z))}} \tag{8}$$
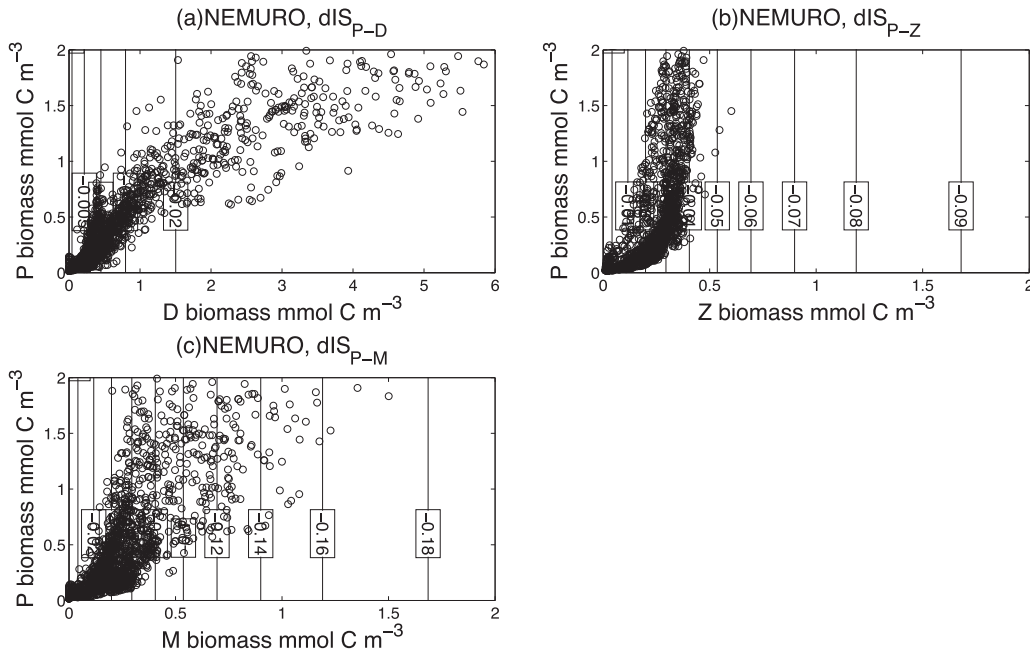

Fig. 9. NEMURO: variation of macrozooplankton biomass (P) with prey biomass (diatoms (D), microzooplankton (Z) and mesozooplankton (M)) in mmol C m^{-3} (circle) and variation of dIS$_{P-prey}$ as a function of the biomass (contour line, in (prey biomass) (predator biomass)$^{-1}$ time^{-1}).
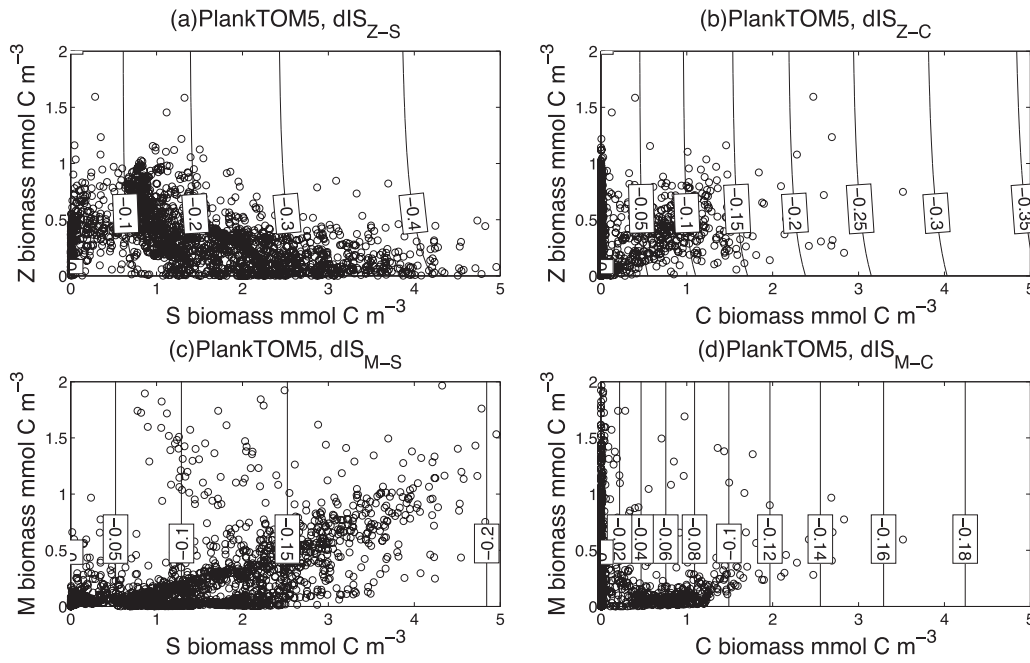
Fig. 10. PlankTOM5: (a) and (b) variation of microzooplankton biomass (Z) with prey biomass (nanophytoplankton (S) and coccolithophores (C)) in mmol C m^{-3} (red circle) and variation of dIS$_{Z-prey}$ as a function of the biomass (contour line, in (prey biomass)(predator biomass)$^{-1}$ time^{-1}). (c) and (d) variation of mesozooplankton biomass (M) with prey biomass (nanophytoplankton (S) and coccolithophores (C)) in mmol C m^{-3} (circle) and variation of dIS$_{M-prey}$ as a function of the biomass (contour line, in (prey biomass)(predator biomass)$^{-1}$ time^{-1}).
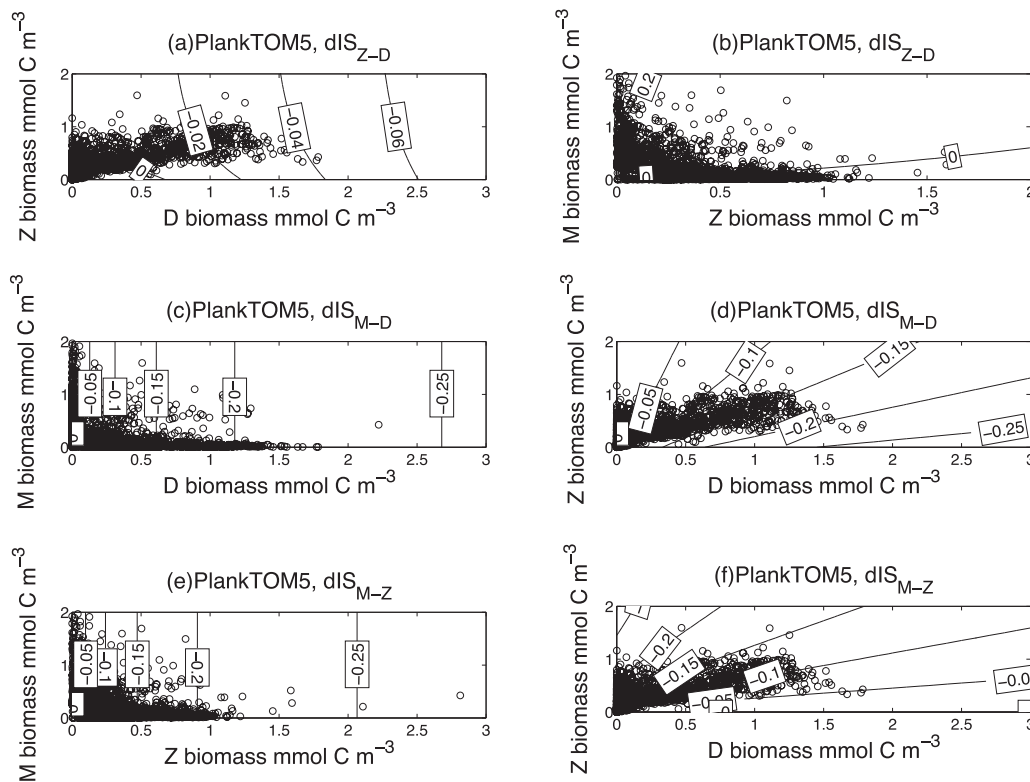

Fig. 11. PlankTOM5: (a) and (b): variation of dIS$_{Z-D}$ (contour line, in (prey biomass)(predator biomass)$^{-1}$ time^{-1}) as a function of masozooplankton (M) and microzooplankton (Z) biomass (a), or microzooplankton and diatoms (D) biomass (in mmol C m^{-3} (b). (c) Variation of dIS$_{M-D}$ (contour line, in (prey biomass)(predator biomass)$^{-1}$ time^{-1}) as a function of mesozooplankton and diatom biomass (circle, in mmol C m^{-3}); (d) variation of dIS$_{M-D}$ (contour line, in (prey biomass)(predator biomass)$^{-1}$ time^{-1}) as a function of microzooplankton and diatom biomass (circle, in mmol C m^{-3}). (e) Variation of dIS$_{M-Z}$ (contour line, in (prey biomass)(predator biomass)$^{-1}$ time^{-1}) as a function of mesozooplankton and microzooplankton biomass (circle, mmol C m^{-3}); (f) variation of dIS^{M-Z} (contour line, in (prey biomass)(predator biomass)$^{-1}$ time^{-1}) as a function of microzooplankton and diatom biomass (circle, mmol C m^{-3}).

Table 3

Value of interaction strength (impact or predator on prey), for all prey–predator prey in each model if biomass of all PFT were to be at their maximal, minimal or median value. '+0' or '−0' value are for interaction strength less than 10^{-4}.

Model	Predator	Prey	Minimal	Maximal	Median
CCSM-BEC	Zooplankton	Nanophytoplankton	−0	−23.7	−7.7
		Diatom	−0.001	−17.8	−2.4
		Diazotroph	−0	−0.21	−0
PISCES	Microzooplankton	Nanophytoplankton	−0.03	−0.23	−0.1
		Diatom	−0.002	−0.61	−0.06
	Mesozooplankton	Nanophytoplankton	−0.02	−0.15	−0.07
		Diatom	−0.001	−0.19	−0.02
		Microzooplankton	−0.002	−0.03	−0.01
NEMURO	Microzooplankton	Nanophytoplankton	+0.023	−0.4	−0.20
		Diatom	+0.001	−0	−0.01
	Mesozooplankton	Nanophytoplankton	+0.006	−0.1	−0.05
		Diatom	+0.022	−0.4	−0.16
		Microzooplankton	+0.017	−0.21	−0.07
	Macrozooplankton	Nanophytoplankton	0	0	0
		Diatom	+0.011	−0	−0.01
		Microzooplankton	+0.009	−0.001	−0.025
		Mesozooplankton	+0.01	−0.17	−0.046
PlankTOM	Microzooplankton	Nanophytoplankton	−0.0001	−0.40	−0.17
		Diatom	−0	+0.024	+0.002
		Coccolithophores	−0	−0.15	−0
	Mesozooplankton	Nanophytoplankton	−0.0004	−0.06	−0.10
		Diatom	−0.0003	−0.09	−0.06
		Coccolithophore	−0.001	−0.04	−0
		Microzooplankton	−0.0008	−0.12	−1.10

The direct interaction expressed in dIS_{Z-D} stands for reduced grazing of diatoms by macrozooplankton with increasing microzooplankton biomass. This term effect is the same as the extra term in dIS_{M-D} and dIS_{M-Z}.

For both microzooplankton and mesozooplankton, their dIS_{zPFT-S} depends on nanophytoplankton biomass only, and at equal prey biomass the maximal dIS is determined by the parameters of the equation (Eqs. (9) and (10)):

$$dIS_{Z-S} = -g_S^Z \left[1 - \frac{1}{e^{(\lambda_Z(S-p2z^*))}} \right] \tag{9}$$

$$dIS_{M-S} = -g_S^M \left[1 - \frac{1}{e^{(\lambda_M(S-p2z^*))}} \right] \tag{10}$$

Microzooplankton biomass increases with nanophytoplankton biomass at low prey levels and then saturates at levels below $0.6 \, mmol \, C \, m^{-3}$, dIS_{Z-S} varies between 0 and −0.4 (Fig. 8a). Mesozooplankton biomass varies with nanophytoplankton in a pattern similar to that of microzooplankton, except that its biomass increases past $0.6 \, mmol \, C \, m^{-3}$; and dIS_{M-S} is between 0 and −0.1 (Fig 8b). At equal nanophytoplankton biomass dIS_{Z-S} is higher than dIS_{M-S} (in term of absolute value). Note that dIS_{P-S} is equal to zero, as there is no direct interaction.

Due to the macrozooplankton grazing formulation (Table 2), dIS_{M-D} and dIS_{M-Z} (Eqs. (11) and (12)) depend on the prey biomass (first term of the equation) and on the biomass of macrozooplankton, mesozooplankton and microzooplankton (second term of the equation).

$$dIS_{M-D} = -g_D^M \left[1 - \frac{1}{e^{(\lambda_M(D-p2z^*))}} + \left[g_D^P P \psi_D \left[1 - \frac{1}{e^{(\lambda_P(D-p2z^*))}} \right] \right] \right]$$
$$\times \frac{1}{e^{(\psi_D(M+Z))}} \tag{11}$$

$$dIS_{M-Z} = -g_Z^M \left[1 - \frac{1}{e^{(\lambda_M(Z-p2z^*))}} + \left[g_Z^P P \psi_Z \left[1 - \frac{1}{e^{(\lambda_P(Z-p2z^*))}} \right] \right] \right]$$
$$\times \frac{1}{e^{(\psi_Z M)}} \tag{12}$$

The variation of mesozooplankton biomass with diatom biomass is similar to that with nanophytoplankton: a linear increase at low

concentration followed by a saturation behavior (Fig. 8c). However, dIS_{M-D} is much stronger with a maximal "absolute" value of −0.35 (−0.09 for dIS_{M-S}). The range of variation of mesozooplankton biomass with microzooplankton biomass (Fig. 8d) is limited by the fact that microzooplankton biomass does not increase past $0.5 \, mmol \, C \, m^{-3}$. dIS_{M-Z} depends on both the predator and prey biomass, with values between 0 and −0.15. dIS_{M-Z} also depends on macrozooplankton biomass (Fig. 8e), and is negative (≥ -0.01) for a macrozooplankton biomass below $1.3 \, mmol \, C \, m^{-3}$. Otherwise, the interaction is positive which means that the increased grazing of mesozooplankton on microzooplankton due to an increase in mesozooplankton biomass is more than compensated for by the reduced macrozooplankton grazing on microzooplankton as the macrozooplankton switch to its preferred prey (mesozooplankton).

Macrozooplankton biomass increases with diatom biomass (Fig. 9a), until diatom biomass reaches about $1 \, mmol \, C \, m^{-3}$, after which macrozooplankton biomass increases more gradually, indicating a tendency towards saturation. The variation of macrozooplankton biomass with microzooplankton biomass (Fig. 9b), or of macrozooplankton biomass with mesozooplankton biomass (Fig. 9c), shows an apparent linear increase of the predator biomass once the prey biomass reaches about $0.3 \, mmol \, C \, m^{-3}$ but with a substantial scatter. dIS_{P-D} is dependent on diatom, microzooplankton and mesozooplankton biomass (Eq. (3)), with mesozooplankton biomass weakening dIS_{P-D} which has values between 0 and −0.025 (Fig. 9a):

$$dIS_{P-D} = -g_D^P \left[1 - \frac{1}{e^{(\lambda_P(D-p2z^*))}} \right] \times \frac{1}{e^{(\psi_D(M+Z))}} \tag{13}$$

Similarly, dIS_{P-Z} depends on microzooplankton and mesozooplankton biomass (Eq. (14)):

$$dIS_{P-Z} = -g_Z^P \left[1 - \frac{1}{e^{(\lambda_P(Z-p2z^*))}} \right] \times \frac{1}{e^{(\psi_Z M)}} \tag{14}$$

Increasing mesozooplankton biomass weakens dIS_{P-Z} while increasing microzooplankton biomass strengthens it. As a result, dIS_{P-Z} varies between 0 and −0.04 (Fig. 9b). dIS_{P-M} depends on

mesozooplankton biomass only (Eq. (15)), and varies between 0 and −0.16 (Fig. 9c), strengthening with mesozooplankton biomass:

$$dIS_{P-M} = -g_M^P \left[1 - \frac{1}{e^{(\lambda_P(M-p2z^*))}} \right] \tag{15}$$

NEMURO dIS$_{predator-prey}$ show a pattern where mesozooplankton is central for transferring lower trophic level carbon to macrozooplankton, while macrozooplankton has a top-down control on the two other zPFTs.

3.3.4. PlankTOM5

Variations of predator biomass with prey biomass are not as clearly correlated in PlankTOM5 as in the other 3 models. There are several possibilities how predator–prey pairs can be related in this model: (i) predator biomass increases with increasing prey biomass (mesozooplankton–nanophytoplankton and microzooplankton–diatoms pairs); (ii) predator and prey are present together for biomass levels below 0.75 mmol C m^{-3} (mesozooplankton–diatom and mesozooplankton–microzooplankton pairs); (iii) appear uncorrelated (microzooplankton–nanophytoplankton pair and coccolithophores as prey). dIS$_{predator-prey}$ values in PlankTOM5 are independent of the predator biomass but, like in PISCES, the formulation for prey preferences creates the possibility for another prey to weaken the dIS. dIS$_{Z-F}$ (Eq. (16)) are primarily dependent on the prey biomass (first term of the equation), then on the biomass of other, additional prey PFTs (second term of the equation), as well as on mesozooplankton biomass.

$$dIS_{Z-F} = -F \frac{g^Z p_F^Z}{k^Z + \sum F p_F^Z} + M F \frac{g^M p_F^M p_Z^M}{(k^M + \sum F p_F^M)^2} \tag{16}$$

The variations of dIS$_{Z-S}$ and dIS$_{Z-C}$ with other prey or mesozooplankton biomass are negligible. dIS$_{Z-S}$ and dIS$_{Z-C}$ only vary with the prey biomass, and increase with increasing prey biomass (Fig. 10a and b). dIS$_{M-F}$ depends on the biomass of the prey and partly on other prey biomass (17).

$$dIS_{M-S} = -F \frac{g^M p_F^M}{k^M + \sum F p_F^M} \tag{17}$$

dIS$_{M-S}$ and dIS$_{M-C}$ effectively depend on prey biomass only, increasing monotonically with increasing prey biomass (Fig. 10c and d). dIS$_{M-S}$ is slightly stronger than dIS$_{M-C}$ (maximal value of −0.2 and −0.14, respectively).

dIS$_{zPFT-D}$ and dIS$_{M-Z}$ depend on more than one prey. dIS$_{Z-D}$ is dependent on the biomass of three PFTs: microzooplankton, diatom and mesozooplankton. dIS$_{Z-D}$ increases (it's value is more negative) with increasing diatom biomass from slightly positive value to −0.06 (Fig. 11a and b for dIS$_{Z-D}$ as a function of microzooplankton and diatoms biomass or mesozooplankton and microzooplankton biomass, respectively). The variation in dIS$_{Z-D}$ as a function of microzooplankton and mesozooplankton biomass ranges between 0.2 and −0.04, with increasing mesozooplankton biomass having a stronger impact on dIS$_{Z-D}$ than microzooplankton biomass (Fig. 11b). Thus the second term of equation 29 is dominant in determining dIS$_{Z-D}$, indicating that variations of microzooplankton biomass have a larger effect on diatoms by modulating mesozooplankton grazing on diatoms. More microzooplankton leads to reduce overall grazing pressure on diatoms.

For microzooplankton and diatoms as prey for mesozooplankton (Fig. 11), the high and equal food preferences of mesozooplankton for both make dIS$_{M-D}$ and dIS$_{M-Z}$ dependent on the biomass of both microzooplankton and diatoms. As a result, dIS$_{M-Z}$ absolute value increases with microzooplankton biomass but decreases with diatom biomass with dIS$_{M-Z}$ values ranging between −0.05 and −0.2 (Fig. 11e and f). The variations and absolute values of dIS$_{M-D}$ are the mirror image of dIS$_{M-Z}$: dIS$_{M-D}$

increases with diatom biomass and decreases with microzooplankton biomass through the same range of value as dIS$_{M-Z}$ (Fig. 11c and d). They vary across a similar range: 0 to −0.20. Microzooplankton and mesozooplankton have strong dIS with one specific pPFT (nanophytoplankton and diatoms, respectively). Mesozooplankton has a strong dIS with both microzooplankton and diatoms to the point where the dIS$_{predator-prey}$ between each predator–prey pair depends strongly on the other prey. This gives an emerging pattern where mesozooplankton can suppress microzooplankton if they are in the same region, with specialization of both predator for a specific prey and different pPFT.

3.4. Specific interaction strength (sIS)

The dIS terms are strongly dependent on prey biomass, which might mask some of the dynamics, so we also calculated specific IS (sIS; Levins, 1964). Specific interactions are obtained in a similar way to direct interactions but using the growth equations divided by the prey biomass (Eq. (18)):

$$sIS_{Y-X} = \frac{\partial}{\partial Y} \left(\frac{1}{X} \frac{\partial X}{\partial t} \right) \tag{18}$$

As a result, the variation of IS$_{predator-prey}$ with prey biomass is reduced or cancelled and will depend on parameter values first, or on other prey biomass.

In CCSM-BEC and NEMURO a dependence of sIS on prey biomass is still present and the scaling of the sIS$_{predator-prey}$ is similar to that of the dIS$_{predator-prey}$ (Fig. 5a and b), showing the dominant interactions within the models. For PISCES and PlankTOM5, the prey biomass dependence is removed from the sIS equation, and sIS$_{predator-prey}$ depends on parameter values (particularly prey preferences) and equation structure (possible prey switching). sIS$_{predator-prey}$ values (Fig. 5b) indicate the preferred food for each predator, in agreement with food preferences. So in PISCES microzooplankton has equal sIS for both nanophytoplankton and diatoms, and mesozooplankton has equal sIS for diatoms and microzooplankton (stronger than sIS$_{M-S}$). In addition, sIS$_{Z-prey}$ values are about three times sIS$_{M-prey}$ values, reflecting the competitive advantage of microzooplankton and the balance between both zPFTs (microzooplankton can graze more but its impact is controlled by mesozooplankton whose weaker IS and maximal grazing rate keep from grazing down a prey). In PlankTOM5, microzooplankton exhibit stronger sIS values for nanophytoplankton than for coccolithophores or diatoms, while mesozooplankton has equal sIS for diatoms and microzooplankton (stronger than sIS$_{M-S}$ and sIS$_{M-C}$). These results underline the degree of specialization of microzooplankton and mesozooplankton for a prey. When added to the strong grazing pressure of mesozooplankton on microzooplankton, it leads to spatial exclusion for the two zPFTs.

4. Discussion

4.1. Intended and obtained food web

Model food webs are built to represent a certain ecosystem as closely as possible to reality. However, the choice of parameters and equations controls the dynamics of the model and how close the obtained dynamics are to the desired ones. Different choices of parameters and functional forms can cause the functional extinction of a PFT (Cropp and Norbury, 2009, 2010) or shape the interactions between PFTs. A chosen set of parameters and equations may cause the obtained food-web to differ from the intended one. Here, we focused on the differences between the intended conceptual food web that led to a specific model formulation, and the resulting food web obtained by the models.
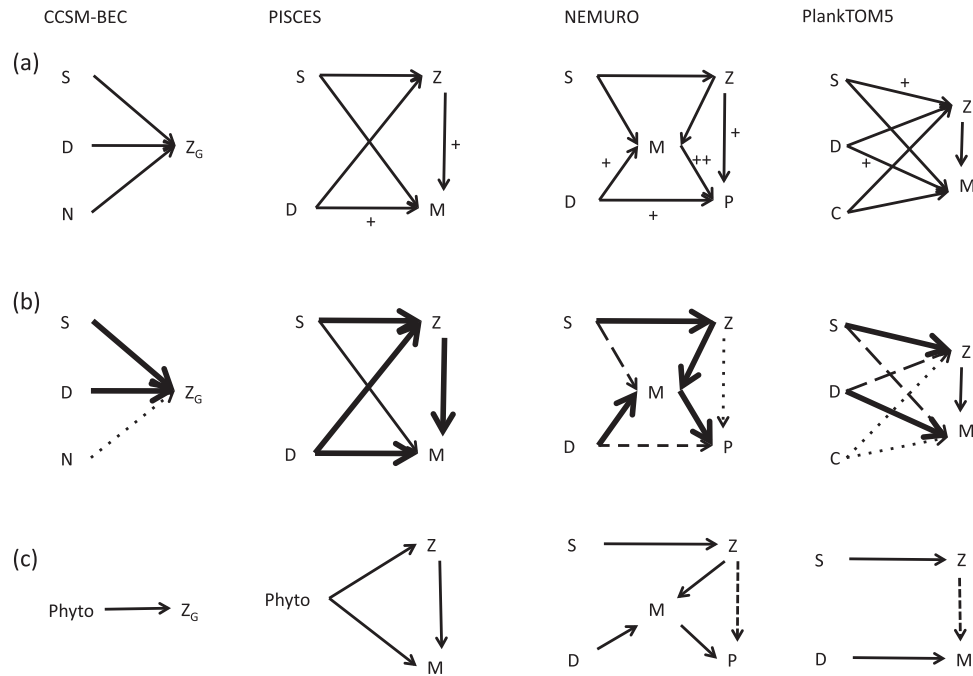
Fig. 12. Schematic of (a) intended food webs with preferred preys, as designed by model equations and parameters identified by a '+', (b) the strong IS are represented by thicker lines, dotted lines are for weak interaction strengths due to low biomass (CCSM-BEC and PlankTOM5) and dashed lines represent weak interaction strengths due to a lack of co-existence of the two PFTs (PlankTOM5) or food preferences (NEMURO); and (c) obtained food webs with dashed arrows representing existing, but weak, interaction between prey and predators. *S*: nanophytoplankton, *D*: diatoms, *C*: coccolithophores, *N*: diazotrophs, Z_G: generic zooplankton in CCSM-BEC, *Z*: microzooplankton, *M*: mesozooplankton and *P*: macrozooplankton.

The intended food web of CCSM-BEC is one of three phytoplankton and one zooplankton (Fig. 12a) with different grazing preferences for each phytoplankton (in order of increasing preference: diazotroph, diatom and nanophytoplankton). The increase in the biomass of one phytoplankton is concurrent with an increase in zooplankton biomass even for diazotrophs, which represent only a small fraction of total phytoplankton biomass. The dIS between the generic zooplankton and an individual pPFT is influenced by the value of the grazing parameters and the biomass of the prey; the strongest interaction occurs for the prey with the highest biomass (fig. 12b). The prey biomass dependence, coupled to the similarity in variation of zooplankton biomass with any of the individual pPFT biomass levels, shows that the effect of CCSM-BEC's generic zooplankton grazing on pPFTs is similar to a density-dependent mortality term. In other words, the pPFTs cannot escape grazing by the generic zooplankton, and blooms are stifled by a strong top-down control (Hashioka et al., under review). As a result it is possible that the advantage of having three different pPFTs, each with a biogeochemical role, is minimized by the lack of variability in pPFTs biomass (less impact on the relevant biogeochemical cycle). Consequently, even if the obtained food-web is the same as the intended one, from a predator–prey interaction point of view it is very close to having one generic phytoplankton and one generic zooplankton (Fig. 12c).

PISCES is designed as a two pPFT, two zPFT food web (Fig. 12a). Microzooplankton exhibits little preference for one pPFT over the other and will prey on the most abundant one. Mesozooplankton has a strong preference for microzooplankton and diatoms, but still preys on the most abundant available prey, so food preferences will influence, but not limit, predation and dIS (Fig. 12b). dIS_{Z-pPFT} and dIS_{M-pPFT} are regulated by the biomass of all PFTs, including mesozooplankton. However, while dIS involving microzooplankton are similar for both pPFTs, mesozooplankton dIS values are more variable and stronger for diatoms and nanophytoplankton, than for microzooplankton. This indicates efficient prey switching by mesozooplankton that will prevent prey extinction in a combination

of top-down and bottom-up control (grazing vs. prey availability). On the other hand, microzooplankton has no food preference and exercise a top-down control on pPFTs while its own biomass is controlled by mesozooplankton. The emergent picture (Fig. 12c) is one with equal preferences on the two pPFTs by both zPFTs, and where mesozooplankton compete with microzooplankton for access to prey, but also prey on microzooplankton, limiting its biomass to a level below its own.

NEMURO's intended food web is one with 2 pPFTs and 3 zPFTs (Fig. 12a). The strong preferences of macrozooplankton for mesozooplankton and microzooplankton over diatoms are reflected in the corresponding dIS values. At the same time, due to biomass effects (e.g. lower biomass of one PFT) mesozooplankton effectively prefers diatoms over microzooplankton. As a result, the dominant interactions are from nanophytoplankton to microzooplankton, from diatoms to mesozooplankton and from mesozooplankton to macrozooplankton (Fig. 12b). Mesozooplankton plays a central role as a link between primary production and macrozooplankton. However, the importance of the biomass of any PFT in modulating dIS is not to be ignored. If mesozooplankton biomass was to become less than that of microzooplankton, the food web would switch to a nanophytoplankton–microzooplankton–macrozooplankton food chain with a weak diatom–macrozooplankton interaction. Such a food web is simulated in high latitude oceans, and favors diatom blooms. The grazing pressures of meso- and macrozooplankton are regulating microzooplankton biomass and keep it at relatively low level (0.5 mmol C m^{-3}). In conclusion, the NEMURO obtained food web is different from the intended one and shaped by macrozooplankton food preferences. Macrozooplankton regulate the biomass of the other two zPFTs, while mesozooplankton channel the production of lower trophic level to macrozooplankton (Fig. 12c). There is a top-down control within zooplankton but not on the phytoplankton, consistent with the results of Hashioka et al. (under review).

PlankTOM5's intended food web includes 3 pPFTs and 2 zPFTs. However, coccolithophores have a minimal importance at a global

scale, and food preferences and interaction strength are such that PlankTOM5's actual food web is different to the one intended (Fig. 12a). The strong preference and dIS of microzooplankton for nanophytoplankton, and of mesozooplankton for diatoms, results in a spatial separation between microzooplankton and mesozooplankton, each dominating in the niche of their preferred prey (Fig. 12b). Additionally, the grazing pressure of mesozooplankton on microzooplankton drives microzooplankton to near extinction, creating a spatial exclusion exacerbated by the prey specialization. This results in an obtained food web that differs greatly from the intended one, with spatially separated communities of small plankton and of larger plankton (Fig. 12c). This accounts for the mix of top-down and bottom-up control of blooms, and the variable bloom composition found by Hashioka et al. (under review).

4.2. Implications

Anderson et al. (2010) changed equations for zooplankton grazing in PlankTOM5 and found that these changes affect the biomass range by up to 50% for all PFTs but not their distribution or community structure. In fact, with any of the four grazing equations examined, they still observe an "inverse relationship" between mesozooplankton and microzooplankton which we labelled "spatial exclusion" in this paper. Anderson et al. (2010) attributed this to microzooplankton being a preferred prey for mesozooplankton, and a top-down control by the latter. However, PISCES has similar equations, food preferences, and intended food web as PlankTOM5, but the relationship between microzooplankton and mesozooplankton is "positive". Within PISCES, there is predation of mesozooplankton on microzooplankton, but both coexist while competing for the two pPFTs. In PlankTOM5 food preferences are expressed more strongly with the result that microzooplankton and mesozooplankton become specialized grazers of one prey, which ultimately enhances the spatial separation that result from grazing of mesozooplankton on microzooplankton.

By comparing PISCES and PlankTOM5, it appears that the choice of parameters for zooplankton has an influence on the impact of zooplankton on the resulting ecosystem, by shaping the food web and modifying the strength of the interactions between prey and predator. This highlights the necessity for well chosen parameters and equations. For a proper choice of parameters and formulations, there is a need for more observations and experiments on zooplankton grazing dynamics and food preferences. Also, data on zooplankton distribution are very dependent on the species or the size class (e.g. copepods have much better data coverage than microzooplankton; Buitenhuis et al., 2006, 2010). The comparison of model output with observations is difficult at present, due to the patchy nature of observations, with the added consideration that PFTs often represent more than one species or taxonomic group of plankton (Buitenhuis et al., 2012). The latter limitations underline the need for more data on zooplankton biomass, distribution, composition, size structure and rates, in order to compare observational data with outputs of models that do not use a generic zooplankton type.

We have shown how predator–prey interactions shape the food-web structure and its dynamics. This is particularly true for the models with two or more zPFT: PISCES, PlankTOM5 and NEMURO. For example, PISCES has a balanced interaction between prey and predators. As such, small changes in biomass (within the model range of biomass) would not affect the dynamics of the food web. Disappearance of one of the pPFTs would change the balance in grazing interaction, increasing the grazing pressure of mesozooplankton on microzooplankton especially if diatoms are the declining pPFT. NEMURO is another example, with its interaction and food web centered around the mesozooplankton even though macrozooplankton is the top predator. Reduction of mesozooplankton

biomass will cause macrozooplankton grazing pressure to shift to microzooplankton and, in an extreme case, toward a nanophytoplankton–microzooplankton–macrozooplankton food chain, instead of the actual food web. These are simple, illustrative examples but one could wonder how much the biomass distribution and results observed in future projections are the result of the external forcing acting on the model food-web dynamics.

Model run for effect of global warming on the marine ecosystem tend to focus on aspect of the ecosystem that are linked to phytoplankton. Future projection runs have found that primary production has variable trends of decrease or increase regionally but will globally decrease (Steinacher et al., 2010), increase in export production (Manizza et al., 2010), an earlier onset of the spring bloom (Hashioka and Yamanaka, 2007), increase in the rate of nitrogen fixation (Boyd and Doney, 2002), and a decrease in diatom linked to increase in stratification (Bopp et al., 2005). However none of these take into account the potential effect of the zooplankton and how its response to global warming.

4.3. Future direction

As stated through this article, the numerical solution of the Jacobian matrix (J) provided us with the value for the direct IS. Comparison of direct IS values and how they are influenced by biomass (prey, predator and other PFTs) informed us on how organisms interact with each other directly. A complementary approach is to look at the negative inverse of the Jacobian matrix ($I = -J^{-1}$; Laska and Wootton, 1998; Montoya et al., 2009). The numerical solutions in the matrix I give the total interaction strength (tIS) between populations. tIS includes the direct interaction strength (dIS), obtained in J, as well as the indirect interaction strength (iIS, e.g. trophic cascades). For example, the direct effect of Z_2 on P (dIS_{Z_2-P}) through grazing is negative, while the indirect effect of Z_2 on P (iIS_{Z_2-P}) through grazing of Z_1 by Z_2 is positive. An approximation is $tIS \approx dIS + iIS$ (Montoya et al., 2009). This approach was considered and preliminary results support our conclusion of the effect induced by prey selection and switching on the food web resulting dynamics. A closer look at the tIS and how it varies with organism biomass, would give useful information on the role and importance of indirect effects in shaping the food-web dynamics (other than food preferences that were visible in the dIS analytical solution).

Another complementary approach would be to look at the systems from the point of view of the resilience and stability of the system and how this can be due to the food web structure and relate to the choice of equations and parameters. In their recent work, Vallina and Le Quéré (2011) explored how model structure influences resilience (capacity to return to the stable state after a perturbation), resistance (strength of the perturbation causing a displacement from the stable state) and stability (distance from the stable state after perturbation). Increased complexity in the model means a decrease in productivity and resilience but a more resistant and stable system. Additionally, the distribution and strength of the interactions are of importance to the stability of the system (Neutel et al., 2002). Lastly, in future work we would like to take into consideration the regional and temporal variability of the model ecosystem and see how the overall food web dynamics impact processes like bloom onset and termination.

5. Conclusion

As demonstrated here, dIS values are dependent on biomass while the chosen parameter values and the equations shape these interactions. It means that the trophic interactions in the model are

ultimately directed by the biomass of the prey or additional prey in the case of a zooplankton with strong food preferences (e.g. Plank-TOM5 and NEMURO). The Jacobian matrix and interaction strength can be used to test the choice of model parameters and equations. In addition, they can assist in an assessment of the type of food web to be expected from a certain set of equations and parameters. The differences between the intended and obtained food webs reflect different existing dynamics, and this is also why none of the models can be considered right or wrong.

The difference in the food web dynamics, highlights the gap in knowledge centered around the zooplankton and predator–prey interactions, it also brings in to question the results of future projections for the marine ecosystems. Reproducing present distributions and biomasses is important, but understanding and duplicating the dynamics that lead to these specific distributions and biomasses is also needed in order to obtain valid projections. In conclusion, we know that models can reproduce different types of food-web dynamics. Understanding them, as well as what they lead to, is an asset for future model development.

Acknowledgment

References

Aita, M.N., Yamanaka, Y., Kishi, M.J., 2007. Interdecadal variation of the lower trophic ecosystem in the north pacific between 1948 and 2002, in 3-d implementation of the nemuro model. Ecological Modeling 202 (1–2), 381–394.

Anderson, T.R., 2005. Plankton functional type modelling: running before we can walk. Journal of Plankton Research 27, 1073–1081.

Anderson, T.R., Gentleman, W.C., Sinha, B., 2010. Influence of grazing formulations on the emergent properties of a complex ecosystem model in a global ocean general circulation model. Progress in Oceanography 87, 201–213.

Aumont, O., Bopp, L., 2006. Globalizing results from ocean in situ iron fertilization studies. Global Biogeochemical Cycles 20, GB2017.

Berlow, E.L., Neutel, A.-M., Cohen, J.E., de Ruiter, P.C., Ebenman, B., Emmerson, M., Fox, J.W., Jansen, V.a.a., Iwan Jones, J., Kokkoris, G.D., Logofet, D.O., McKane, A.J., Montoya, J.M., Petchey, O., 2004. Interaction strengths in food webs: issues and opportunities. Journal of Animal Ecology 73 (May (3)), 585–598, http://dx.doi.org/10.1111/j.0021-8790.2004.00833.x, ISSN 0021-8790.

Bopp, L., Aumont, O., Cadule, P., Alvain, S., Gehlen, M., 2005. Response of diatoms distribution to global warming and potential implications: a global model study. Geophysics Research Letters 32, L19606, http://dx.doi.org/10.1029/2005GL023653.

Boyd, P.W., Doney, S.C., 2002. Modelling regional responses by marine pelagic ecosystems to global climate change. Geophysical Research Letters 29 (16), 1016.

Buitenhuis, E.T., Le Quéré, C., Aumont, O., Beaugrand, G., Bunker, A., Hirst, A., Ikeda, T., O'Brien, T., Piontkovski, S., Straile, D., 2006. Biogeochemical fluxes through mesozooplankton. Global Biogeochemical Cycles 20, GB2003.

Buitenhuis, E.T., Rivkin, R.B., Sailley, S., Le Quéré, C., 2010. Biogeochemical fluxes through microzooplankton. Global Biogeochemical Cycles 24, GB4015.

Buitenhuis, E.T., Vogt, M., Moriarty, R., Swan, C., Bednarsek, N., Doney, S., Leblanc, K., Le Quéré, C., Luo, Y., O'Brien, C., O'Brien, T., Peloquin, J., Schiebel, R., Swan, C., 2012. MAREDAT: towards a world ocean atlas of marine ecosystem data. Earth System Science Data Discussions 5, 1077–1106.

Cropp, R., Norbury, J., 2009. Parameterizing plankton functional type models: insight from a dynamical systems perspective. Journal of Plankton Research 31 (9), 939–963.

Cropp, R., Norbury, J., 2010. Parameterising competing zooplankton for survival in plankton functional type models. Ecological Modelling 221, 1852–1864.

Doney, S.C., Fabry, V.J., Feely, R.A., Kleypas, J.A., 2009a. Ocean acidification: the other CO$_2$ problem. Annual Review of Marine Science 1, 169–192.

Doney, S.C., Lima, I., Moore, J.K., Lindsay, K., Behrenfeld, M.J., Westberry, T.K., Mahowald, N., Glover, D.M., Takahashi, T., 2009b. Skill metrics for confronting global upper ocean ecosystem-biogeochemistry models against field and remote sensing data. Journal of Marine Systems 76, 95–112.

Doney, S.C., Ruckelshaus, M., Duffy, J.E., Barry, J.P., Chan, F., English, C.A., Galindo, H.M., Grebmeier, J.M., Hollowed, A.B., Knowlton, N., Polovina, J., Rabalais, N.N., Sydeman, W.J., Talley, L.D., 2012. Climate impacts on marine ecosystem dynamics. Annual Review of Marine Science 4, 11–37.

Falkowski, P., Scholes, R.J., Boyle, E., Canadell, J., Canfield, D., Elser, J., Gruber, N., Hibbard, K., Hogberg, P., Linder, S., Mackenzie, F.T., Pedersen, B.M.III.T., Rosenthal, Y., Seitzinger, S., Smetacek, V., Steffen, W., 2000. The global carbon cycle: a test of our knowledge of earth as a system. Science 290, 291.

Fasham, M.J.R., Sarmiento, J.L., Slate, R.D., Ducklow, H.W., Williams, R., 1993. Ecosystem behavior at bermuda station "s" and ocean weather station "India": a general circulation model and observational analysis. Global Biogeochemical Cycles 7 (2), 379–415.

Fussmann, G.F., Balsius, B., 2005. Community response to enrichment is highly sensitive to model structure. Biology Letters 1, 9–12.

Gentleman, W.C., Leising, A., Frost, B., Strom, S., Murray, J., 2003. Functional responses for zooplankton feeding on multiple resources: a review of assumptions and biological dynamics. Deep-Sea Research II 50, 2847–2875.

Hashioka, T., Vogt, M., Yamanaka, Y., Le Quéré, C., Aita, M.N., Alvain, S., Bopp, L., Hirata, T., Lima, I., Sailley, S., Doney, S.C., Phytoplankton competition during the spring bloom in four plankton functional type models. Biogeosciences, under review.

Hashioka, T., Yamanaka, Y., 2007. Ecosystem change in the western North Pacific associated with global warming obtained by 3-D NEMURO. Ecological Modeling 202 (1–2), http://dx.doi.org/10.1016/j.ecolmodel.2006.05.038.

Kishi, M.J., Kashiwai, M., Ware, D.M., Megrey, B.A., Eslinger, D.L., Werner, F.E., Noguchi-Aita, M., Azumaya, T., Fujii, M., Hashimoto, S., Huang, D., Iizumi, H., Ishida, Y., Kang, S., Kantakov, G.A., cheol Kim, H., Komatsu, K., Navrotsky, V.V., Smith, S.L., Tadokoro, K., Tsuda, A., Yamamura, O., Yamanaka, Y., Yokouchi, K., Yoshie, N., Zhang, J., Zuenko, Y.I., Zvalinsky, V.I., 2007. Nemuro – a lower trophic level model for the north pacific marine ecosystem. Ecological Modelling 202, 12–25.

Laska, M.S., Wootton, J.T., 1998. Theoretical concept and empirical approached to measuring interaction strength. Ecology 79 (2), 461–476.

Le Quéré, C., Harrison, S.P., Prentice, I.C., Buitenhuis, E.T., Aumont, O., Bopp, L., Claustre, H., da Cunha, L.C., Geider, R., Giraud, X., Klaas, C., Kohfeld, K.E., Legendre, L., Manizza, M., Platt, T., Rivkin, R.B., Sathyendranath, S., Uitz, J., Watson, A.J., Wolf-Gladrow, D., 2005. Ecosystem dynamics based on plankton functional types for global ocean biogeochemistry models. Global Change Biology 11, 2016–2040.

Levins, R., 1964. Evolution in Changing Environments. Princeton University Press, Princeton, NJ.

Manizza, M., Le Quéré, C., Buitenhuis, E.T., 2010. Sensitivity of global ocean biogeochemical dynamics to ecosystem structure in a future climate. Geophysics Research Letters 37, L13607.

May, R.M., 1974. Stability and Complexity in Model Ecosystems. Princeton University Press, Princeton, NJ.

Montoya, J.M., amd Mark, G.W., Emmerson, C., Solé, R.V., 2009. Press perturbations and indirect effects in real food webs. Ecology 90 (9), 2426–2433.

Moore, J., Doney, S.C., Lindsay, K., 2004. Upper ocean ecosystem dynamics and iron cycling in a global three-dimensional model. Global Biogeochemical Cycles 18, GB4028.

Neutel, A.-M., Heesterbeek, J.A.P., de Ruiter, P.C., May 2002. Stability in real food webs: weak links in long loops. Science 296, 1120–1123.

Steinacher, M., Joos, F., Frölicher, T.L., Bopp, L., Cadule, P., Cocco, V., Doney, S.C., Gehlen, M., Lindsay, K., Moore, J.K., Schneider, B., Segschneider, J., 2010. Projected 21st century decrease in marine productivity: a multi-model analysis. Biogeosciences 7, 979–1005, http://dx.doi.org/10.5194/bg-7-979-2010.

Vallina, S.M., Le Quéré, C., 2011. Stability of complex food webs: resilience, resistance and the average interaction strength. Journal of Theoretical Biology 272, 160–173.

Vogt, M., Hashioka, T., Le Quéré, C., Alvain, S., Bopp, L., Buitenhuis, E.T., Doney, S.C., Lima, I., Aita, M.N., Yamanaka, Y., MARine Ecosystem Model Inter-comparison Project (MAREMIP): the representation of ecological niches in different Dynamic Green Ocean Models, in preparation.

Woods, S.N., Thomas, M.B., 1999. Super-sensitivity to structure in biological models. Proceedings of the Royal Society, London B 266, 565–570.

Wootton, J.T., Emmerson, M., 2005. Measurement of interaction strength in nature. Annual Review of Ecology, Evolution, and Systematics 36, 419–444.